Advanced Fiber Materials (2019) 1:188–196
https://doi.org/10.1007/s42765-019-00010-1

RESEARCH ARTICLE

Cellulose Nanofibrous Membranes Modified with Phenyl Glycidyl Ether for Efficient Adsorption of Bovine Serum Albumin

Lihuan Wang[1] · Qiuxia Fu[1] · Jianyong Yu[1,2] · Lifang Liu[1] · Bin Ding[1,2]

Received: 23 July 2019 / Accepted: 23 August 2019 / Published online: 23 September 2019

Abstract

Hydrophobic interaction chromatography (HIC) as an indispensable method for protein purification has attracted considerable attentions of researchers as well as biopharmaceutical industries. However, the low binding capacity and slow adsorption rate of the currently available HIC media lead to a little supply and high price of the highly purified proteins. Herein, nanofibrous membranes with hydrophobic binding sites were developed for HIC by directly coupling phenyl glycidyl ether on the hydrolyzed cellulose acetate nanofiber membrane (cellulose-phenyl NFM). Scanning electron microscope (SEM), water contact angle (WCA), Fourier transform infrared (FTIR), thermogravimetric analysis (TGA), Brunauer–Emmett–Teller (BET) surface area analysis and capillary flow porometer (CFP) were applied to evaluate the physically and chemically structural transformation. The obtained cellulose-phenyl NFMs showed a proper hydrophilcity (WCA = 37°), a relatively high BET surface area (3.6 times the surface area of commercial fibrous membranes), and tortuous-channel structure with through-hole size in the range of 0.25–1.2 μm, which led to a little non-specificity adsorption, high bovine serum albumin adsorption capacity of 118 mg g^{-1}, fast adsorption process within 12 h, good long-term stability and reusability. Moreover, compared with traditional modification methods which always include activation and graft two steps, direct coupling method is more efficient for HIC media fabrication. Therefore, cellulose-phenyl NFMs with outstanding protein adsorption performance could be a kind of promising candidate for HIC.

Graphic Abstract

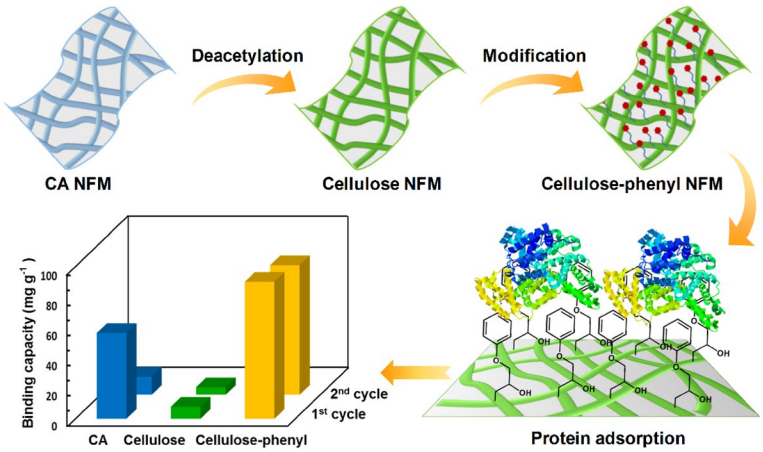

Keywords Cellulose nanofibers · Phenyl glycidyl ether · Protein adsorption · Hydrophobic interaction chromatography

Electronic supplementary material The online version of this article (https://doi.org/10.1007/s42765-019-00010-1) contains supplementary material, which is available to authorized users.

Extended author information available on the last page of the article

Introduction

Separation and purification of proteins are mostly performed by chromatography owing to its high efficiency and high resolution [1]. Hydrophobic interaction chromatography (HIC) as a complementary to ion exchange and affinity chromatography, which separates proteins with minimum protein structural denaturation, has been regard as a powerful method for protein separation both in laboratory and industry [2]. Conventional HIC columns for bio-separation are packed with porous resin beads or gel microspheres modified with butyl, hexyl, octyl or phenyl groups. These media are incapable of meeting large quantities of separation due to their inherent deficiencies, such as the slow adsorption rate, low flow rate and large dosage of solvent consumption caused by diffusion type and internal binding sites.

Porous membranes as a kind of promising chromatography media have shown great preponderances. One of the most important superiority of membrane chromatography is that the mass transfer resistance is reduced when compared to beads-packed column chromatography, which boosts the adsorption rate and reduces the buffer usage [3–6]. These advantages make membrane chromatography much more attractive these years. Polyvinylidene fluoride microporous membranes applied for purification of monoclonal antibody, chimeric heavy chain monoclonal antibody, human plasma proteins, mono-PEGylated lysozyme, immunoglobulin G and its subclasses have been reported by Ghosh and coworkers, implying that membranes could be a kind of cost-effective media for protein HIC with high efficiency [7–15]. Moreover, filter papers modified with polyethylene glycol, poly-(*N*-isopropylacrylamide)-butyl-acrylate or poly (*N*-vinyl caprolactam) were also developed as HIC media [6, 16, 17]. These filter paper-based HIC media could allow the flow flux of the mobile phase being heavily improved. Although HIC membranes have been in existence for quite a while, the limited binding capacity of these membranes caused by the relatively small specific surface area restricts their practical applications [18–20].

Nanofiber-assembled membranes possess highly tortuous porous structure, large specific surface area, and robust mechanical strength [21–23], which could elevate the immobilization efficiency, long-term stability and reusability, are expected to be ideal substitutes to porous resin beads and microporous membranes for immobilization of ligands and capturing protein.

Here we propose a novel kind of HIC media based on phenyl-modified electrospun nanofibrous membranes (NFMs). Cellulose nanofiber membrane is designed as the matrix for its large surface area, low nonspecific adsorption feature and excellent corrosion stability [24, 25]. However, the fabrication of cellulose nanofibers by electrospinning directly is difficult due to the insolubility of cellulose in common solvents. To overcome this disadvantage, we prepared the electrospinning cellulose acetate (CA) NFMs as the pre-matrix, and then hydrolyzed the CA NFMs to cellulose NFMs for phenyl grafting by direct coupling method. In comparison to traditional modification methods which always include activation and graft two steps, direct coupling method is more efficient for HIC media fabrication. To the best of our knowledge, though electrospun NFMs as protein adsorbents based on affinity and ion-exchange have been developed [26–28], there is fewer reported work on applying phenyl group modified cellulose NFMs for proteins adsorption based on hydrophobic interaction. The resultant cellulose-phenyl NFMs showed excellent adsorption performance, involving high bovine serum albumin (BSA) binding capacity, rapid adsorption rate, and favorable reusability. It is expected that these HIC media made in the present work could meet the efficient adsorption of proteins.

Experimental Section

Preparation of Cellulose-Phenyl NFMs

The CA solution was prepared by dissolving 7.5 g CA powder (Mw = 30,000, acetyl content of 40%) in 42.5 g DMAc/acetone (1/2, w/w) mixture solvent with a vigorous stir of 12 h. The electrospinning was performed under a voltage of 20 kV, a flow rate of 0.5 ml h^{-1}, a spinneret-to-collector distance of 15 cm, temperature of 25 ± 5 °C, and relative humidity of 45 ± 5%. Afterword, the obtained CA NFMs were hydrolyzed in 0.2 M NaOH aqueous solution at 50 °C for 5 h to get the cellulose NFMs. Subsequently, the cellulose NFMs were washed with deionized water, and then were dehydrated by the mixed solvent of acetone/water with gradient ratios (1/3, 2/2, 3/1, 4/0). The modification of cellulose NFMs with phenyl glycidyl ether (PGE) was performed as follows: 10 ml cellulose NFMs were immersed into 20 ml dioxane with 1 ml PGE, followed by adding 0.1 g $BF_3{\cdot}Et_2O$ as catalyst. The PGE ring-open reaction was taken place at 45 °C, 30 min. Finally, the obtained cellulose-phenyl NFMs were washed with acetone/water (3/1, 2/2, 1/3, 0/4) and dried at 60 °C for 4 h in the oven.

Protein Adsorption Experiment

The protein adsorption experiment was performed by immersing 0.02 g cellulose-phenyl NFMs in 4 ml of 1 mg ml^{-1} BSA solution with 2 mmol ml^{-1} $(NH_4)_2SO_4$ (pH = 7) for 24 h. The effects of pH value (5, 6, 7, 8 and

9), $(NH_4)_2SO_4$ concentration (0, 0.5, 1.0, 1.5, 1.75 and 2 mmol ml^{-1}), and BSA concentration (0.2, 0.4, 0.6, 0.8 and 1.0 mg ml^{-1}) on the adsorption performance were also investigated. The reusability of the cellulose-phenyl NFMs was realized by washing the fibrous membranes with PBS five times after each adsorption. The BSA concentration of the solution was detected by ultraviolet–visible (UV–vis) spectrophotometer (at 277 nm).

Characterization

The microstructure of the NFMs was characterized by scanning electron microscope (SEM, TM 3000). The thermal property was performed by thermogravimetric analysis (TGA). Fourier transform infrared spectroscopy (FTIR) was used to characterize the chemical structure of the samples. The water contact angle (WCA) was measured by contact angle measuring device. The Brunauer–Emmett–Teller (BET) surface area was characterized by the surface area analyzer (ASAP2020). The through-hole size distribution was analyzed by capillary flow porometer. The pH value of protein solution was tested by pH meter (PHS-3C).

Results and Discussion

Chromatographic media are always washed by corrosive solutions, therefore, the materials should have good chemical stability to resist harsh conditions. Additionally, nonspecific adsorption should be minimized since the nonspecific adsorption can compromise the purification efficiency. Cellulose is a commonly used matrix for its good chemical stability and low nonspecific adsorption feature. However, it is difficult to be dissolved in the general solvents, leading to the fabrication of electrospun cellulose nanofiber membranes difficult. Herein, CA NFMs were firstly fabricated by electrospinning, and then they were deacetylated to cellulose NFMs by NaOH solution. The cellulose-phenyl NFMs applied for protein adsorption based on hydrophobic interaction were got by further modifying the cellulose NFMs with PGE (Scheme 1).

The Physical and Chemical Structure of Cellulose-Phenyl NFMs

The morphological changes of NFMs caused by hydrolysis and grafting reactions were shown in Fig. 1a–d. The CA NFMs exhibited smooth fiber surface, and the average fiber diameter was 245 nm. Notwithstanding that CA is a kind of hydrophilic polymer, the CA NFMs showed a WCA of

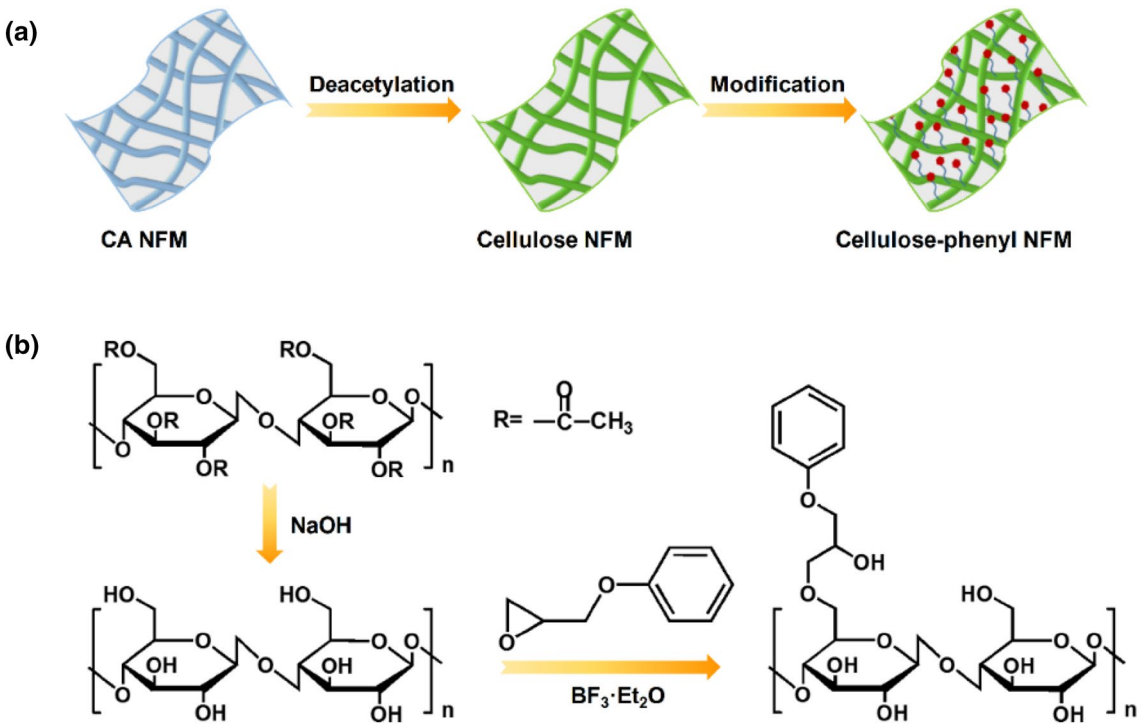

Scheme 1 **a** The schematic illustration of cellulose-phenyl NFM fabrication process and **b** the chemical reactions during this procedure

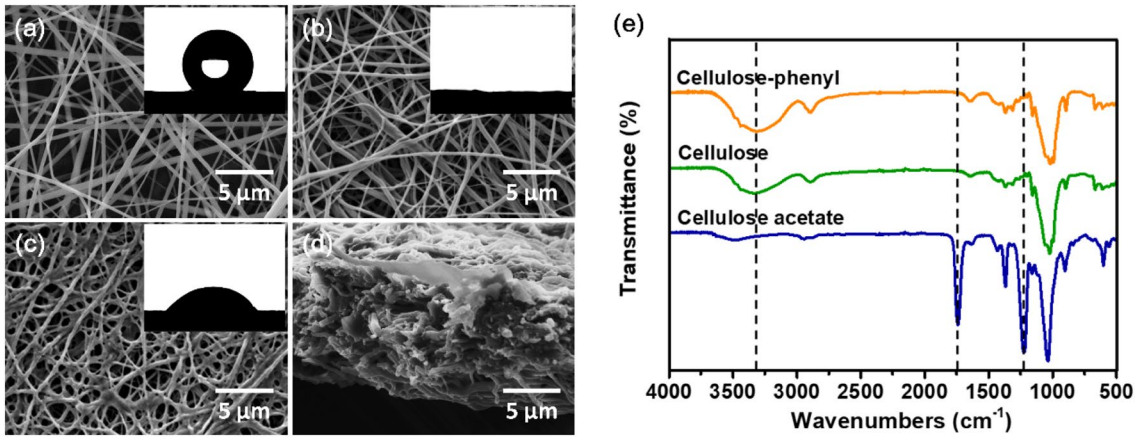

Fig. 1 SEM images and WCAs of **a** CA, **b** cellulose, **c** cellulose-phenyl NFMs, and **d** cross-section SEM image of cellulose-phenyl NFMs. **e** FTIR spectra of CA, cellulose and cellulose-phenyl NFMs

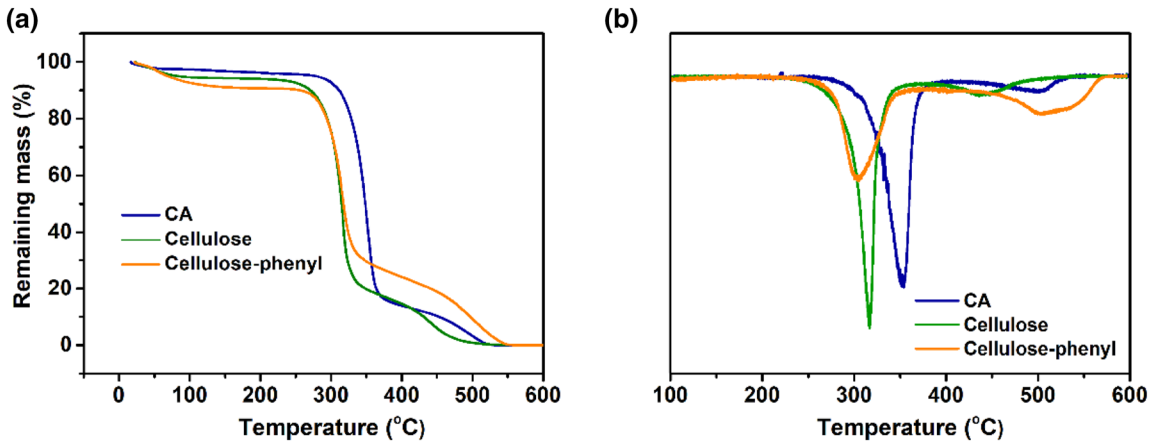

Fig. 2 **a** TG and **b** DTG traces of CA, cellulose and cellulose-phenyl NFMs

130° due to the influence of acetyl group and hierarchical nanofibrous structure [29]. Upon being deacetylated in 0.2 M NaOH solution at 50 °C, the acetyl groups gradually converted to hydroxyl groups, leading to the obtained cellulose NFMs with a larger average fiber diameter of 269 nm and super hydrophilicity. The FTIR analysis also confirmed that CA transferred to cellulose. As shown in Fig. 1e, FTIR characteristic peaks of CA such as alkoxyl stretch of ester at 1223 cm^{-1} and vibrations of acetyl groups at 1725 cm^{-1} completely disappeared after hydrolysis. On the contrary, the peak at 3325 cm^{-1} corresponding to the vibration of –OH increased sharply. After PGE modification, bonding points among fibers appeared in the cellulose-phenyl NFMs (Fig. 1c). Nevertheless, the tortuous channels still existed in the cellulose-phenyl NFMs (Fig. 1d). The WCA of cellulose-phenyl NFMs was 37°, indicating the wettability had a little change after modification of phenyl group. Whereas, no new peaks appeared after coupling with phenyl groups, which may attribute to the weak stretching and relatively low percent grafting of phenyl group [30].

Table 1 Thermogravimetric parameters during the second weight loss of all samples

Samples	CA	Cellulose	Cellulose-phenyl
T_{start} (°C)	257	226	233
T_{max} (°C)	354	316	303
T_{end} (°C)	377	357	350
Wight loss ratio (%)	80	76	62

The changes of chemical structure were further confirmed by pyrolysis analysis. The thermogravimetric (TG) curves and the first derivative of the TG (DTG) curves in Fig. 2 showed that the pyrolysis processes of all samples include three stages: loss of moisture, degradation of the polymer

chains, and decomposition of glucosyl. Parameters including temperature of samples starting to decompose (T_{start}), temperature of the maximum degradation reaction rate (T_{max}) and temperature of the decomposition end (T_{end}) deduced from the TG and DTG curves were shown in Table 1. For CA, 80.0% weight loss happened at 257–377 °C and the maximum mass loss rate was at 354 °C. Compared to CA NFMs, degradation of cellulose NFMs occurred at a lower temperature range (226–357 °C), which was also reported by Zhou et al. [31]. The corresponding decompose temperature of cellulose-phenyl NFMs was in the range of 233–350 °C, quite near to that of cellulose NFMs. Nevertheless, since Lewis acid catalyst is very aggressive to cause more or less undesired degradation of cellulose during phenyl modification [32], the T_{max} (303 °C) of cellulose-phenyl is a little lower than that of cellulose (316 °C). Interestingly, the degradation of cellulose-phenyl NFMs at the third stage was in a higher temperature range (450–550 °C) when compared to that of CA (450–520 °C) and cellulose (400–470 °C), which may attribute to the aromatization of charred residues [33].

Surface area and porous structure, including mesoporous and through channels of NFMs, are the vital factors that greatly affected the protein binding capacity and drop pressure. The N_2 adsorption and desorption curves in Fig. 3a revealed that there was no mesoporous on the nanofiber surface, thus the pore diffusion of proteins could be avoided, and the adsorption and desorption time could be reduced. The BET surface area of CA, cellulose, and cellulose-phenyl NFMs was 4.18, 3.45, and 2.95 $m^2\ g^{-1}$, respectively. The decrease of the cellulose NFMs surface area may be due to the increased fiber diameter, while the decrease of the cellulose-phenyl NFMs surface area may attribute to the adhesion structure among fibers (Fig. 1c). Even though, the surface area of cellulose-phenyl NFMs was still much superior to that of commercial fibrous membranes (0.81 $m^2\ g^{-1}$) [20]. The through hole size distributions tested by capillary flow porometer showed that the average pore size decreased from 1.8 to 0.5 μm after deacetylation and modification (Fig. 3b), which may attribute to the increased packing density and adhesion structure in cellulose-phenyl NFMs.

Protein Adsorption Behavior of Cellulose-Phenyl NFMs

To get a deep insight into the adsorption behavior, adsorption experiments under different conditions were performed. Comparative adsorption test of CA, cellulose and cellulose-phenyl NFMs were firstly performed to analyze the effect of chemical structure. The UV-spectra in Fig. 4a showed that the CA NFMs had a BSA binding capacity of 57 mg g^{-1} due to the hydrophobic acetyl groups. In contrast, quiet few proteins have been adsorbed on cellulose NFMs. This is because the superhydrophilic hydroxyl groups covered on the cellulose are protein resistant. After modified with hydrophobic phenyl groups, the binding capacity of cellulose-phenyl NFMs reached 91 mg g^{-1}, and this result can be attributed to the phenyl groups which played as hydrophobic binding sites for protein capturing. The FTIR in Figure S1 showed that after adsorption of BSA, spectrum peaks at 3189 and 3022 cm^{-1} attributed to the vibrations of N–H, and peaks at 1409 and 1049 cm^{-1} corresponding to the vibrations of C–N appeared, indicating BSA has been adsorbed on the cellulose-phenyl NFMs. Though the CA NFMs can adsorb proteins as well, it is nonspecific adsorption and not conducive to protein separation. We confirmed the nonspecific adsorption of CA NFMs by comparing the binding capacities between the first and second adsorptions. As shown in Fig. 4b, the binding capacities of cellulose and cellulose-phenyl NFMs after the second adsorption had no obvious change, indicating their nonspecific adsorption was not

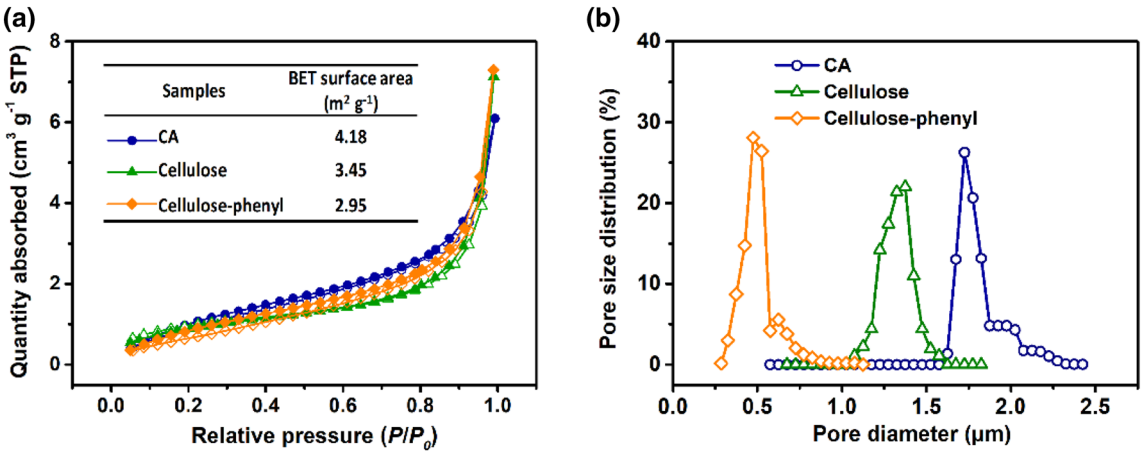

Fig. 3 **a** N_2 adsorption–desorption curves and **b** through hole size distributions of CA, cellulose and cellulose-phenyl NFMs tested by capillary flow porometer

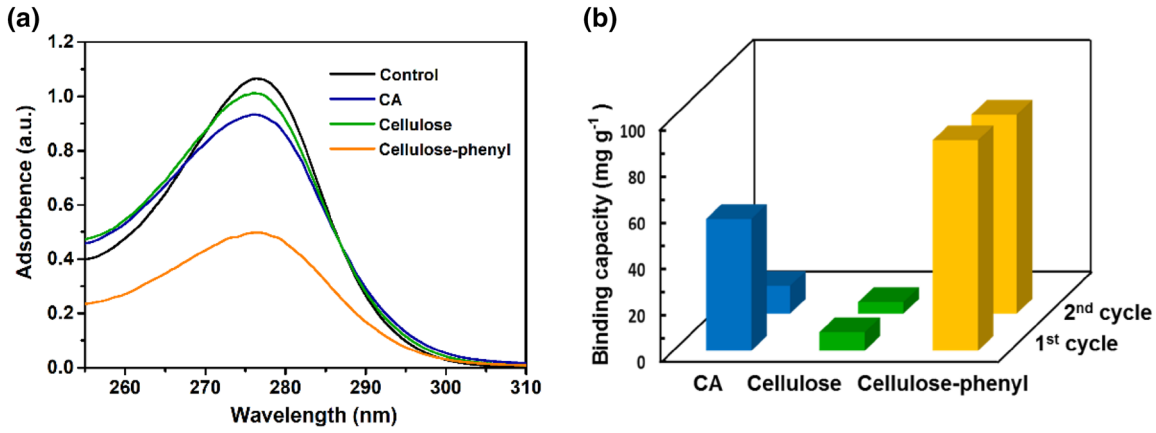

Fig. 4 **a** UV–vis spectra of the BSA solutions after being adsorbed by CA, cellulose and cellulose-phenyl NFMs respectively, and **b** the BSA binding capacities [in 1 mg ml^{-1} BSA, 2 mmol ml^{-1} $(NH_4)_2SO_4$, pH = 7] of various NFMs in first and the second cycle

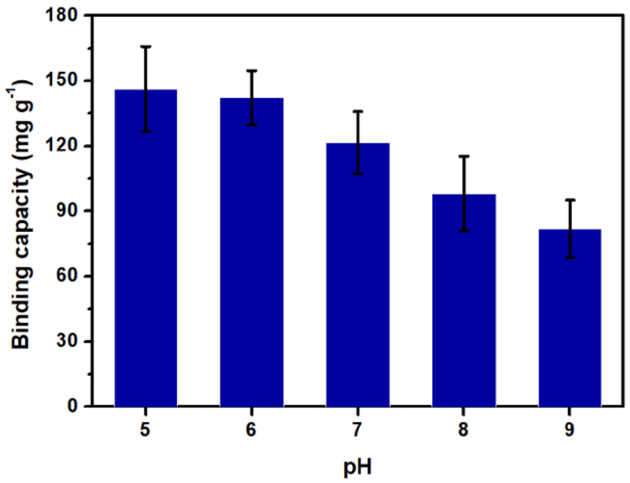

Fig. 5 The effect of pH value on BSA binding capacity [in 1 mg ml^{-1} BSA, 2 mmol ml^{-1} $(NH_4)_2SO_4$] of cellulose-phenyl NFMs

serious. However, the binding capacity of CA NFMs in the second cycle decreased heavily, illustrating the hydrophobic binding sites were occupied by proteins adsorbed in the first cycle and could not be eluted by PBS. Therefore, cellulose-phenyl NFMs with low nonspecific adsorption are favorable to protein separation.

Since pH value can affect the protein binding capacity via influencing the net charge and charge distribution of proteins, BSA binding capacities of cellulose-phenyl NFMs at various pH values were assayed. The experimental results showed that the BSA binding capacity decreased as the pH value increasing from 5 to 9 (Fig. 5). This phenomenon can be explained as follows: when the pH value was close to the isoelectric point of BSA (4.7), the net charge was about zero and hydrophobic interactions reached maximum. As the pH value increasing, the positive net charge of BSA increased, which led to the electrostatic interaction between proteins and cellulose-phenyl NFMs enhanced. As a result, the hydrophobic interactions between proteins and cellulose-phenyl NFMs reduced. Even though, the differences of BSA binding capacities at various pH values were not huge when compared to that of ion-exchange adsorption. Considering the BSA binding capacity at pH = 5 was the highest, thus pH = 5 was selected for the following experiments.

Salt concentration is another critical factor that greatly influences the protein binding capacity, therefore the research of ionic strength on the adsorption behaviors has become the most intriguing field in the studies of protein HIC. Based on the solvophobic theory [34], the presence of lyotropic salts enhances the surface tension of salt solution and brings the entropy down. For the sake of offsetting the entropy, the bound form of protein is more stable than the unbound protein thermodynamically. For this reason, the protein binding capacity is favored at high salt concentration. Given that the salt concentration should be lower than the concentration which could cause protein precipitation, the concentration of $(NH_4)_2SO_4$ is not exceeded 2.0 M. The experiment data in Fig. 6a showed that the surface tension of the $(NH_4)_2SO_4$ solution was enhanced as salt content increasing, resulting in a more hydrophobic condition for both proteins and cellulose-phenyl NFMs. As a result, the BSA binding capacity at all protein concentrations increased exponentially as the $(NH_4)_2SO_4$ increasing (Fig. 6b).

Adsorption kinetics can provide valuable data for understanding the mechanism of mass transfer and adsorption procedure. To elucidate the kinetic behavior of cellulose-phenyl NFMs, adsorption experiment was performed by prolonging the adsorption time. As displayed in Fig. 7a, the UV-spectral absorption peak at 277 nm decreased as time going on and kept mostly unchangeable when over 12 h, indicating the cellulose-phenyl NFMs possessed a fast adsorption process due to the absence of internal diffusion resistance [35]. The adsorption process could be divided into two stages and

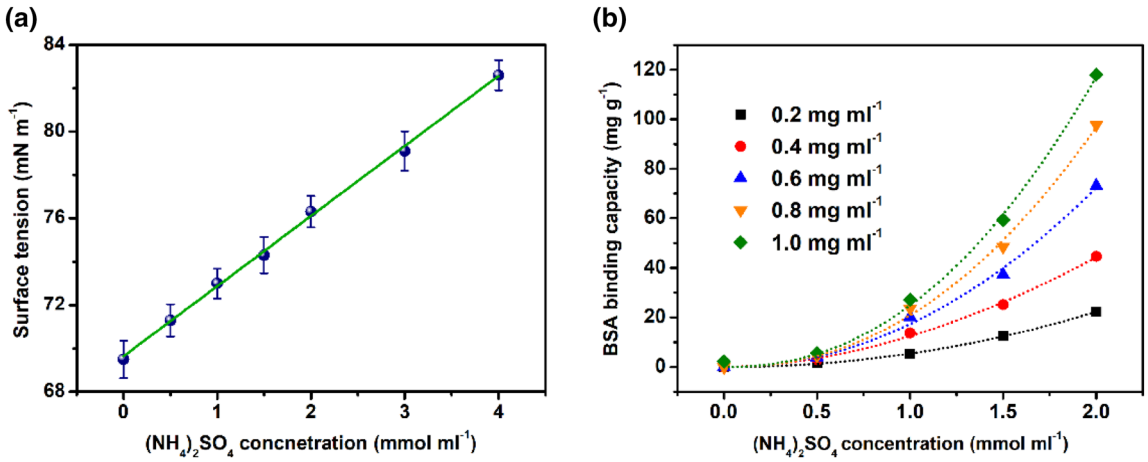

Fig. 6 **a** The solution surface tension and as the concentration of $(NH_4)_2SO_4$ increasing. **b** The BSA binding capacity of cellulose-phenyl NFMs in solutions with various BSA and $(NH_4)_2SO_4$ concentrations (pH = 5)

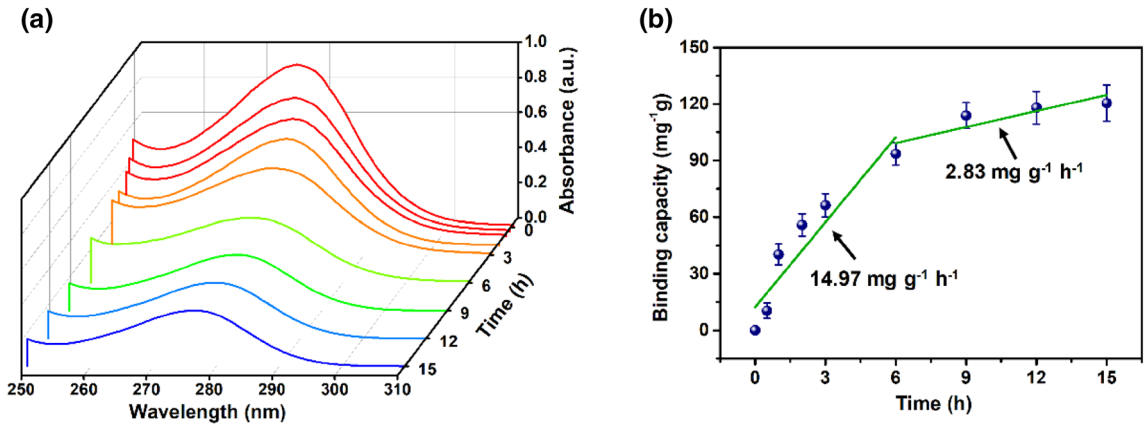

Fig. 7 **a** UV–vis spectra of the BSA solutions as the adsorption time going on. **b** The liner fitting plot of the binding capacity [in 1 mg ml^{-1} BSA, 2 mmol ml^{-1} $(NH_4)_2SO_4$, pH = 5] at two stages

linearly fitted to predict the adsorption rate (Fig. 7b). At the first 6 h, the cellulose-phenyl NFMs possessed a high average adsorption rate of 14.97 mg g^{-1} h^{-1}. As time prolonging, the gap of protein concentration between the mobile phase and solid phase decreased, which led to the adsorption rate falling to 2.83 mg g^{-1} h^{-1}.

Additionally, taking the economic plausibility and practicability into consideration, the reusability of the adsorbent is required. The reusability of the cellulose-phenyl NFMs was investigated by washing the fibrous membranes with PBS three times after each adsorption to elute the adsorbed BSA, and the schematic was shown in Fig. 8a. Subsequently, the regenerated cellulose-phenyl NFMs were reused for another cycle. The binding capacities of 10 cycles showed in Fig. 8b had little difference, and the nanofibrous morphology still existed after the 10th treatment (Fig. 8c). For dynamic adsorption test, cellulose-phenyl NFMs with a total thickness of 2 mm were packed in a syringe, and 1 mg ml^{-1} BSA solution was poured into the syringe and flowed through the NMFs. The dynamic binding capacity of cellulose-phenyl NFMs calculated from the dynamic breakthrough curve (Fig. S2) was 24.7 mg ml^{-1}. Furthermore, the chemical stability of cellulose-phenyl was proved by adsorption BSA after harsh acid and alkali treatment (immersing in pH = 2 HCl or pH = 13 NaOH solution with 2 h). The binding capacities after acid and alkali treatment (112 and 109 mg g^{-1}, respectively) had no significant changes.

Conclusions

In conclusion, nanofibrous membrane media for protein adsorption were successfully prepared by directly coupling phenyl groups on cellulose NFMs. The BSA binding capacity of these NFMs was affected by $(NH_4)_2SO_4$ concentration, pH value, and protein concentration. As the concentration

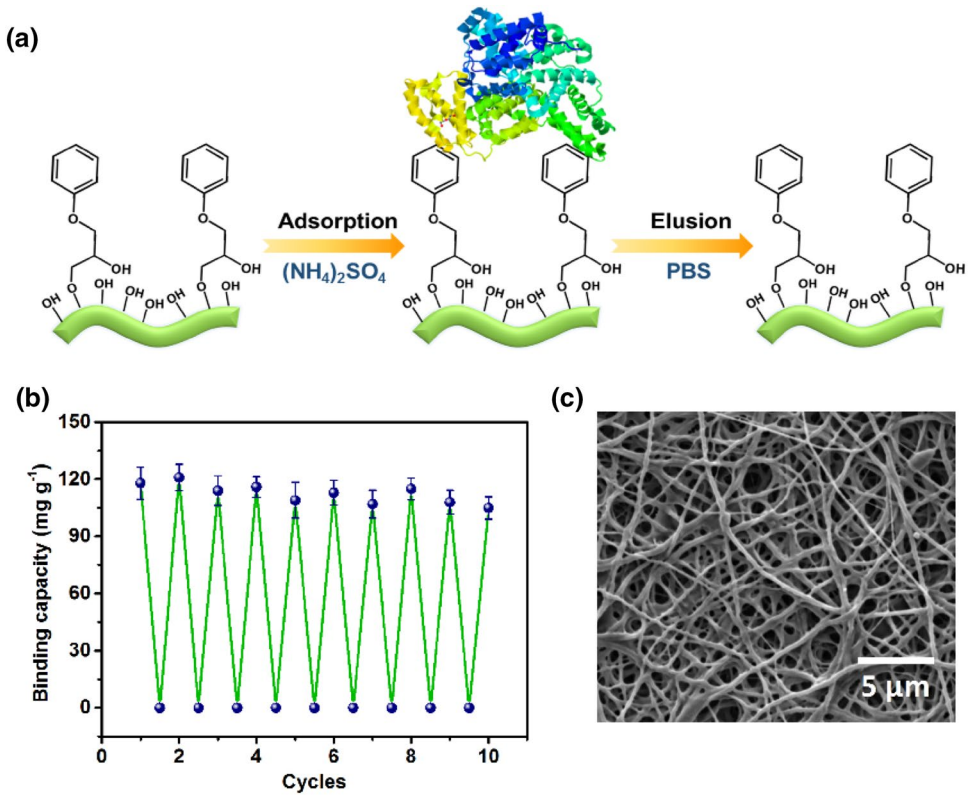

Fig. 8 **a** The scheme of protein adsorption and elution. **b** The reusability of cellulose-phenyl NFMs with 10 cycles and **c** the SEM image of cellulose-phenyl NFMs after 10 cycles

of $(NH_4)_2SO_4$ or protein increasing, BSA binding capacity increased. The pH value closed to the isoelectric point was conducive to protein adsorption. The static adsorption capacity can reach as high as 118 mg g^{-1} when the solution contained 1 mg ml^{-1} BSA and 2 mmol ml^{-1} $(NH_4)_2SO_4$, pH = 5. Additionally, the cellulose-phenyl NFMs exhibit rapid adsorption rate, good chemical resistant and reusability. Therefore, cellulose-phenyl NFMs with outstanding protein adsorption performance could be a kind of competitive HIC media for protein purification.

Acknowledgements This work was supported by the National Natural Science Foundation of China (Grant Nos. 51673037, 51873029, and 81771338), and the Science and Technology Commission of Shanghai Municipality (Grant No. 18511109500).

Compliance with ethical standards

Conflict of interest The authors declare no conflicts of interest.

References

1. Jungbauer A. Chromatographic media for bioseparation. *J Chromatogr A*. **2005**;*1065*:3.
2. Chen B, Peng Y, Valeja SG, Xiu L, Alpert AJ, Ge Y. Online hydrophobic interaction chromatography-mass spectrometry for top-down proteomics. *Anal Chem*. **2016**;*88*:1885.
3. Kawai T, Saito K, Lee W. Protein binding to polymer brush, based on ion-exchange, hydrophobic, and affinity interactions. *J Chromatogr B Anal Technol Biomed Life Sci*. **2003**;*790*:131.
4. Ghosh R. Separation of proteins using hydrophobic interaction membrane chromatography. *J Chromatogr A*. **2001**;*923*:59.
5. Chang CS, Suen SY. Modification of porous alumina membranes with n-alkanoic acids and their application in protein adsorption. *J Membr Sci*. **2006**;*275*:70.
6. Yu D, Chen X, Pelton R, Ghosh R. Paper-PEG-based membranes for hydrophobic interaction chromatography: purification of monoclonal antibody. *Biotechnol Bioeng*. **2008**;*99*:1434.
7. Ghosh R, Wang L. Purification of humanized monoclonal antibody by hydrophobic interaction membrane chromatography. *J Chromatogr A*. **2006**;*1107*:104.
8. Ghosh R. Fractionation of human plasma proteins by hydrophobic interaction membrane chromatography. *J Membr Sci*. **2005**;*260*:112.
9. Huang R, Mah KZ, Malta M, Kostanski LK, Filipe CDM, Ghosh R. Chromatographic separation of proteins using hydrophobic membrane shielded with an environment-responsive hydrogel. *J Membr Sci*. **2009**;*345*:177.
10. Yu D, Ghosh R. Integrated fragmentation of human IgG and purification of fab using a reactant adsorptive membrane bioreactor separator system. *Biotechnol Bioeng*. **2009**;*104*:152.
11. Wang L, Ghosh R. Feasibility study for the fractionation of the major human immunoglobulin G subclasses using hydrophobic interaction membrane chromatography. *Anal Chem*. **2010**;*82*:452.
12. Yu D, Shang X, Ghosh R. Fractionation of different PEGylated forms of a protein by chromatography using environment-responsive membranes. *J Chromatogr A*. **2010**;*1217*:5595.
13. Yoo SM, Ghosh R. Simultaneous removal of leached protein-A and aggregates from monoclonal antibody using

hydrophobic interaction membrane chromatography. *J Membr Sci*. **2012**;*390*:263.
14. Shang X, Wittbold W, Ghosh R. Purification and analysis of mono-PEGylated HSA by hydrophobic interaction membrane chromatography. *J Sep Sci*. **2013**;*36*:3673.
15. Sadavarte R, Spearman M, Okun N, Butler M, Ghosh R. Purification of chimeric heavy chain monoclonal antibody EG2-hFc using hydrophobic interaction membrane chromatography: an alternative to protein-A affinity chromatography. *Biotechnol Bioeng*. **2014**;*111*:1139.
16. Mah KZ, Ghosh R. Paper-based composite lyotropic salt-responsive membranes for chromatographic separation of proteins. *J Membr Sci*. **2010**;*360*:149.
17. Wu Q, Wang R, Chen X, Ghosh R. Temperature-responsive membrane for hydrophobic interaction based chromatographic separation of proteins in bind-and-elute mode. *J Membr Sci*. **2014**;*471*:56.
18. Chiu HT, Lin JM, Cheng TH, Chou SY. Fabrication of electrospun polyacrylonitrile ion-exchange membranes for application in lysozym. *Express Polym Lett*. **2011**;*5*:308.
19. Jones TT, Fernandez EJ. Hydrophobic interaction chromatography selectivity changes among three stable proteins: conformation does not play a major role. *Biotechnol Bioeng*. **2004**;*87*:388.
20. Kosior A, Antosova M, Faber R, Villain L, Polakovic M. Single-component adsorption of proteins on a cellulose membrane with the phenyl ligand for hydrophobic interaction chromatography. *J Membr Sci*. **2013**;*442*:216.
21. Cui FH, Li Y, Zhao X, Yin X, Yu J, Ding B. Multilevel porous structured polyvinylidene fluoride/polyurethane fibrous membranes for ultrahigh waterproof and breathable application. *Comput Commun*. **2017**;*6*:63.
22. Ding XX, Li Y, Si Y, Yin X, Yu JY, Ding B. Electrospun polyvinylidene fluoride/SiO2 nanofibrous membranes with enhanced electret property for efficient air filtration. *Comput Commun*. **2019**;*13*:57.
23. Hua T, Li Y, Zhao X, Yin X, Yu JY, Ding B. Stable low resistance air filter under high humidity endowed by self-emission far-infrared for effective PM 2.5 capture. *Comput Commun*. **2017**;*6*:29.
24. Ma JC, Wang XQ, Fu QX, Si Y, Yu JY, Ding B. Highly carbonylated cellulose nanofibrous membranes utilizing maleic anhydride grafting for efficient lysozyme adsorption. *ACS Appl Mater Interfaces*. **2015**;*7*:15658.
25. Zhang LF, Menkhaus TJ, Fong H. Fabrication and bioseparation studies of adsorptive membranes/felts made from electrospun cellulose acetate nanofibers. *J Membr Sci*. **2008**;*319*:176.
26. Che AF, Huang XJ, Xu ZK. Polyacrylonitrile-based nanofibrous membrane with glycosylated surface for lectin affinity adsorption. *J Membr Sci*. **2011**;*366*:272.
27. Fu QX, Wang XQ, Si Y, Liu LF, Yu JY, Ding B. Scalable fabrication of electrospun nanofibrous membranes functionalized with citric acid for high-performance protein adsorption. *ACS Appl Mater Interfaces*. **2016**;*8*:11819.
28. Fu QX, Duan C, Yan ZS, Si Y, Liu LF, Yu JY, Ding B. Electrospun nanofibrous composite materials: a versatile platform for high efficiency protein adsorption and separation. *Comput Commun*. **2018**;*8*:92.
29. Ogawa T, Ding B, Sone Y, Shiratori S. Super-hydrophobic surfaces of layer-by-layer structured film-coated electrospun nanofibrous membranes. *Nanotechnology*. **2007**;*18*:165607.
30. Dods SR, Hardick O, Stevens B, Bracewell DG. Fabricating electrospun cellulose nanofibre adsorbents for ion-exchange chromatography. *J Chromatogr A*. **2015**;*1376*:74.
31. Zhou B, Li Y, Deng HB, Hu Y, Li B. Antibacterial multilayer films fabricated by layer-by-layer immobilizing lysozyme and gold nanoparticles on nanofibers. *Colloid Surface B*. **2014**;*116*:432.
32. Arndt P, Bockholt K, Gerdes R, Huschens S, Pyplo J, Redlich H, Samm K. Cellulose oligomers: preparation from cellulose triacetate, chemical transformations and reactions. *Cellulose*. **2003**;*10*:75.
33. Singh R, Arora S, Lal K. Thermal and spectral studies on cellulose modified with various cresyldichlorothiophosphates. *Thermochim Acta*. **1996**;*289*:9.
34. Chen J, Sun Y. Modeling of the salt effects on hydrophobic adsorption equilibrium of protein. *J Chromatogr A*. **2003**;*992*:29.
35. Mak S, Chen D. Fast adsorption of methylene blue on polyacrylic acid-bound iron oxide magnetic nanoparticles. *Dyes Pigments*. **2004**;*61*:93.

Affiliations

Lihuan Wang[1] · Qiuxia Fu[1] · Jianyong Yu[1,2] · Lifang Liu[1] · Bin Ding[1,2]

✉ Lifang Liu
lifangliu@dhu.edu.cn

✉ Bin Ding
binding@dhu.edu.cn

[1] State Key Laboratory for Modification of Chemical Fibers and Polymer Materials, College of Textiles, Donghua University, Shanghai 201620, China

[2] Innovation Center for Textile Science and Technology, Donghua University, Shanghai 200051, China